

---

# Scalability of Atomic-Thin-Body (ATB) Transistors Based on Graphene Nanoribbons

Qin Zhang<sup>1</sup>, Yeqing Lu<sup>1</sup>, Huili Grace Xing<sup>1</sup>, Steven J. Koester<sup>2</sup>, and Siyuranga O. Koswatta<sup>3</sup>

<sup>1</sup>Department of Electrical Engineering, University of Notre Dame, Notre Dame, IN 46556, USA

Tel: (574) 631-5498, Fax: (574) 631-4393, email: [qzhang1@nd.edu](mailto:qzhang1@nd.edu)

<sup>2</sup>University of Minnesota, 200 Union St. SE, Minneapolis, Twin Cities, MN 55455, USA

<sup>3</sup>IBM Research Division, T. J. Watson Research Center, Yorktown Heights, NY 10598, USA

## Abstract

A general solution for the electrostatic potential in an atomic-thin-body (ATB) field-effect transistor geometry is presented. The effective electrostatic scaling length,  $\lambda_{eff}$ , is extracted from the analytical model, which cannot be approximated by the lowest order eigenmode as traditionally done in SOI-MOSFETs. An empirical equation for the scaling length that depends on the geometry parameters is proposed. It is shown that even for a thick SiO<sub>2</sub> back oxide  $\lambda_{eff}$  can be improved efficiently by thinner top oxide thickness, and to some extent, with high-k dielectrics. The model is then applied to self-consistent simulation of graphene nanoribbon (GNR) Schottky-barrier field-effect transistors (SB-FETs) at the ballistic limit. In the case of GNR SB-FETs, for large  $\lambda_{eff}$ , the scaling is limited by the conventional electrostatic short channel effects (SCEs). On the other hand, for small  $\lambda_{eff}$ , the scaling is limited by direct source-to-drain tunneling. A subthreshold swing below 100mV/dec is still possible with a sub-10nm gate length in GNR SB-FETs.

---

***Index Terms*** – Graphene, Schottky-barrier, thin-body, transistor scaling, subthreshold swing.

---

## I. INTRODUCTION

Graphene has been attracting considerable attention as an alternative channel material to silicon in CMOS technology [1]-[6] because of its remarkable electrical properties [1] as well as due to the fact that an energy band gap can be induced under certain conditions in this normally gapless material [2]-[4]. Therefore, it may be possible to realize atomic-thin-body (ATB) transistors based on graphene. To date, GNR based transistor operation has been numerically simulated using the nonequilibrium Green's function formalism combined with 3D electrostatics [5]-[6]. A generalized scaling theory for the ATB field-effect transistor (ATB-FET) geometry however, has not been presented, which is different from the well established ultrathin-body (UTB) structures which have comparatively large body thicknesses with a well-defined semiconductor dielectric medium [7]-[9]. In this letter, a new generalized analytical solution is derived to calculate the electrostatic potential in the ATB-FET geometry which is applicable to transistors based on single-layer and few-layer graphene as well as conventional semiconductor materials with body thicknesses below  $\sim 1\text{nm}$  [10]. On the other hand, carrier transport properties will depend on the individual bandstructure of the specific material. Here, we simulate GNR based Schottky-barrier FETs (SB-FETs) to explore their scalability dependence on geometrical parameters.

## II. APPROACH

The structure of a double-gate (DG) ATB transistor is illustrated in Fig. 1(a). The atomic thin channel material with a length  $L_g$  and a negligible thickness (assumed to be zero in the model) is placed in between the top and back oxides. The top oxide has a thickness of  $t_{tox}$  and dielectric constant of  $\epsilon_{tox}$ , and the back oxide is  $\text{SiO}_2$  ( $\epsilon_{box} = 3.9\epsilon_0$ ) with a thickness of  $t_{box}$ . The potential boundary conditions are as shown in Fig. 1(a).

It should be noted that due to the negligible body thickness of ATB-FETs the parabolic approximation for the potential across the body cannot be used here as was done in original scaling studies [11]-[12]. Therefore, we use a procedure similar to that in [7]-[9], whereby the electrostatic potential of the ATB-FET can be written as  $\psi(x, y) = v(x) + ul(x, y) + ur(x, y)$ , where  $v(x)$  is the long-channel solution that accounts for the top and bottom boundary conditions, as well as the self-consistent charge induced in the channel (therefore, the solution is valid in both subthreshold as well as above-threshold operation).  $ul(x, y)$  and  $ur(x, y)$  satisfy the source and drain boundary conditions, respectively, and can be expanded as:

$$ul(x, y) = \begin{cases} \sum_{n=1}^{\infty} A_n^l \frac{\sin[k_n(x + t_{tox})]}{\sin(k_n t_{tox})} \frac{\sinh[k_n(L_g - y)]}{\sinh(k_n L_g)} (-t_{tox} \leq x \leq 0) \\ \sum_{n=1}^{\infty} -A_n^l \frac{\sin[k_n(x - t_{box})]}{\sin(k_n t_{box})} \frac{\sinh[k_n(L_g - y)]}{\sinh(k_n L_g)} (0 \leq x \leq t_{box}) \end{cases} \quad (1)$$

$$ur(x, y) = \begin{cases} \sum_{n=1}^{\infty} A_n^r \frac{\sin[k_n(x + t_{tox})]}{\sin(k_n t_{tox})} \frac{\sinh(k_n y)}{\sinh(k_n L_g)} (-t_{tox} \leq x \leq 0) \\ \sum_{n=1}^{\infty} -A_n^r \frac{\sin[k_n(x - t_{box})]}{\sin(k_n t_{box})} \frac{\sinh(k_n y)}{\sinh(k_n L_g)} (0 \leq x \leq t_{box}) \end{cases} \quad (2)$$

where the eigenvalues  $\lambda_n = 1/k_n$  are determined by the implicit equation,  $\varepsilon_{box} \tan(k_n t_{tox}) + \varepsilon_{tox} \tan(k_n t_{box}) = 0$ . The coefficients  $A_n^l$  and  $A_n^r$  are calculated by integrating  $ul(x, 0) * g_n(x)$  and  $ur(x, L_g) * g_n(x)$  from  $-t_{tox}$  to  $t_{box}$ , respectively, where  $g_n(x)$  is constructed to be a set of corresponding conjugate functions to each term in  $ul(x, 0)$  that satisfies  $\int_{-t_{tox}}^{t_{box}} ul_n(x, 0) g_m(x) dx = \delta_{n,m}$  (note that  $g_n(x)$  will simultaneously satisfy a similar condition with each term of  $ur(x, L_g)$  as well). The calculated eigenvalues  $\lambda_n$  and coefficients  $A_n^l, A_n^r$  are shown in Fig. 1(b). Using the above series solution, an effective scaling length ( $\lambda_{eff}$ ) is extracted by an exponential fitting of the potential profile near the source region. Since the eigenmodes are

weighted by the expansion coefficients  $A_n^l$  and  $A_n^r$ , which do not necessarily peak at  $n = 1$  (Fig. 1(b)),  $\lambda_{eff}$  cannot be approximated by the first eigenvalue ( $\lambda_1$ ) as has been traditionally done in SOI-MOSFETs [7]-[9]. For the geometry considered in Fig. 1(b) the first eigenvalue gives  $\lambda_1 \approx 16\text{nm}$ , which shows a large discrepancy to the 2D series solution with  $\lambda_{eff} \approx 1.6\text{nm}$ .

We use the above series solution to simulate GNR SB-FETs, considering a 2nm-wide GNR with an energy band gap of  $E_g = 0.69\text{eV}$  [13], and source/drain SB height of  $\Phi_B = 0.1\text{V}$ . The Schottky barrier and direct source-to-drain (S $\rightarrow$ D) tunneling are both included on the same footing, whereby the WKB tunneling coefficient is calculated using the imaginary bandstructure of the GNR that treats the electron-hole nature of carriers realistically. Ballistic transport simulations are performed similar to [14] accounting for self-consistent electrostatics, while any edge-induced states in the band gap [15] and phonon scattering [16] are not considered.

### III. RESULTS AND DISCUSSION

Figure 2(a) compares the extracted  $\lambda_{eff}$  to the lowest order eigenvalue  $\lambda_1$  as a function of  $t_{tox}$  for different  $t_{box}$  values. It is clearly seen that  $\lambda_1$  cannot correctly describe  $\lambda_{eff}$ . Therefore, an

empirical equation  $\lambda_{emp} = \alpha t_{tox} \left[ 1 + \frac{\epsilon_{box}}{\epsilon_{tox}} \right] \left[ 1 + \left( \frac{\epsilon_{box}}{\epsilon_{tox}} \right) \left( \frac{t_{tox}}{t_{box}} \right) \right] / \left[ 1 + \frac{t_{tox}}{t_{box}} \right]$  is proposed to

approximate  $\lambda_{eff}$ , and this equation shows reasonable consistency for a large range of  $t_{tox}$  and  $\epsilon_{tox}$  values at thick SiO<sub>2</sub> box limit where  $\alpha = 0.6$  is the only fitting parameter (Fig. 2). It is seen in Fig. 2(a) that  $\lambda_{eff}$  is greatly improved by thinner  $t_{tox}$ , and also modulated by  $t_{box}$  when it is below a certain thickness ( $< 50\text{ nm}$ ). On the other hand,  $\lambda_{eff}$  and  $\lambda_{emp}$  do not appreciably depend on  $t_{box}$  for thicknesses  $> 50\text{nm}$ . Figure 2(b) plots  $\lambda_{eff}$  as a function of  $\epsilon_{tox}$  for different  $t_{tox}$ , and shows that  $\lambda_{eff}$  is also improved by high-k top oxide, but the improvement saturates at a certain point [5] [7]. More importantly, even for a thick SiO<sub>2</sub> back oxide,  $\lambda_{eff}$  can be reduced below 2nm by thinning the top oxide thickness.

---

The transfer characteristics of GNR SB-FETs are shown in Fig. 3(a) for different gate lengths. For the calculated geometry,  $I_{on}/I_{off} > 10^3$  is achieved at a supply voltage of 0.3V. Figures 3(b) and 3(c) show the band diagram and the energy-resolved current density in the off-state of the  $L_g = 10\text{nm}$  and  $15\text{nm}$  devices, respectively. For this geometry which has  $\lambda_{eff} = 1.45\text{nm}$ , when the channel length is  $L_g \geq 15\text{nm}$  the subthreshold swing ( $SS$ ) approaches the  $60\text{mV}/\text{dec}$  limit, but it degrades to  $85\text{mV}/\text{dec}$  at  $L_g = 10\text{nm}$  because of direct  $S \rightarrow D$  tunneling (Fig. 3(b)). Here, we extract the  $SS$  values where  $\log_{10}(I_D) - V_{GS}$  is nearly linear in Fig. 3(a) at  $V_{GS} \approx 0.05\text{V}$ . In order to further elucidate the scaling potential of GNR SB-FETs, Fig. 4(a) plots  $SS$  vs.  $L_g$ , and Fig. 4(b) plots  $SS$  vs.  $L_g/(\pi\lambda_{eff})$ . Since the 2D potential at the middle of the channel near the thermionic barrier region depends on  $\exp(-L_g/2\lambda_{eff})$ , previous works [7] [9] [12] have shown that  $SS$  degrades significantly for  $L_g/(\pi\lambda_{eff}) \leq 1.5 \sim 2$  due to excessive thermal leakage.

We, however, identify two distinct limiting conditions for  $SS$  degradation depending on the device geometrical parameters that are yet practically relevant: 1) for very small  $\lambda_{eff}$  values,  $SS$  degradation is mainly due to direct  $S \rightarrow D$  tunneling, while 2) at larger  $\lambda_{eff}$ ,  $SS$  degradation is due to conventional electrostatic short-channel-effects (SCEs) [7] [9] [12]. For thin  $t_{tox}$  ( $1\text{nm}$  and  $2.15\text{nm}$ ) in Fig. 4(a) with small  $\lambda_{eff}$ ,  $SS$  degradation for  $L_g$  below  $\sim 15\text{nm}$  is due to direct  $S \rightarrow D$  tunneling [5], and not because of electrostatic SCEs. An  $SS \leq 100\text{mV}/\text{dec}$  is still possible for sub- $10\text{nm}$   $L_g$  with small  $\lambda_{eff}$  values, even though obtaining small off-state currents will be a challenge because of the direct tunneling limit. Nevertheless, narrower GNRs with larger band gaps may alleviate this problem [5]. For thick  $t_{tox}$  ( $5\text{nm}$  and  $8\text{nm}$ ) in Fig. 4(b), on the other hand, with large  $\lambda_{eff}$ ,  $SS$  increases to  $\sim 100\text{mV}/\text{dec}$  when the conventional  $L_g/(\pi\lambda_{eff}) \approx 1.5$  condition is met [7] [9] [12]. In other words, in the large  $\lambda_{eff}$  limit, scaling is controlled by the electrostatic SCEs. Interestingly, when comparing Fig. 2 with SOI-MOSFET simulations in [9] for a similar device

---

geometry, the GNR channel has smaller  $\lambda_{eff}$  than the 5nm thick Si based UTB channel, showing the excellent scaling potential of GNR based ATB-FETs.

#### IV. CONCLUSIONS

A generalized 2D analytical electrostatic solution is developed for the ATB-transistor geometry. An empirical equation for the effective scaling length has been proposed which cannot be approximated by the lowest order eigenmode as traditionally done in SOI-MOSFETs. Even for a thick SiO<sub>2</sub> back oxide, the scaling length can be efficiently improved by thinner top oxide, and to some extent, by high-k dielectrics. It is seen that the scalability of GNR SB-FETs can be limited either by direct S→D tunneling, or conventional electrostatic SCEs, depending on the geometrical parameters. Compared to conventional UTB-FET geometries, excellent scaling potential of ATB-FETs based on graphene has been demonstrated.

---

## REFERENCES

- [1] A. K. Geim, "Graphene: status and prospects," *Science*, vol. 324, pp.1530-1534, 2009.
- [2] M. C. Lemme, T. J. Echtermeyer, M. Baus, and H. Kurz, "A graphene field-effect device," *IEEE Electron Dev. Lett.*, vol. 28, no. 4, pp. 282-284, 2007.
- [3] Z. Chen, Y. -M. Lin, M. J. Rooks, and P. Avouris, "Graphene nano-ribbon electronics," *Physica E*, vol. 40, pp. 228-232, 2007.
- [4] E. McCann, "Asymmetry gap in the electronic band structure of bilayer graphene," *Phys. Rev. B*, vol. 74, no. 16, p. 161403, 2006.
- [5] Y. Ouyang, Y. Yoon, and J. Guo, "Scaling behaviors of graphene nanoribbon FETs: a three-dimensional quantum simulation study," *IEEE Trans. Electron Dev.*, vol. 54, no. 9, pp. 2223-2231, 2007.
- [6] G. Fiori and G. Iannaccone, "Simulation of graphene nanoribbon field-effect transistors," *IEEE Electron Dev. Lett.*, vol. 28, no.8, pp. 760-762, 2007.
- [7] D. J. Frank, Y. Taur, and H. -S. P. Wong, "Generalized scale length for two-dimensional effects in MOSFETs," *IEEE Electron Dev. Lett.*, vol. 19, no. 10, pp. 385-387, 1998.
- [8] S. -H. Oh, D. Monroe, J. M. Hergenrother, "Analytic description of short-channel effects in fully depleted double-gate and cylindrical, surrounding-gate MOSFETs," *IEEE Electron Dev. Lett.*, vol. 21, no. 9, pp. 445-447, 2000.
- [9] X. Liang and Y. Taur, "A 2-D analytical solution for SCEs in DG MOSFETs," *IEEE Trans. Electron Dev.*, vol. 51, no. 8, pp. 1385-1391, 2004.
- [10] M. Schmidt, M. C. Lemme, H. D. B. Gottlob, F. Driussi, L. Selmi, and H. Kurz, "Mobility extraction in SOI MOSFETs with sub 1 nm body thickness," *Solid-State Electronics*, vol. 53, no. 12, pp. 1246-1253, 2009.

- 
- [11] K. K. Young, "Short-channel effect in fully depleted SOI MOSFETs," *IEEE Trans. Electron Dev.*, vol. 36, no. 2, pp. 399-402, 1989.
- [12] R. H. Yan, A. Ourmazd, and K. F. Lee, "Scaling the Si MOSFET – from bulk to SOI to bulk," *IEEE Trans. Electron Dev.*, vol. 39, no. 11, pp. 1704-1710, 1992.
- [13] B. Trauzettel, D. V. Bulaev, D. Loss, and G. Burkard, "Spin qubits in graphene quantum dots," *Nature Phys.*, vol. 3, pp. 192-196, 2007.
- [14] L. C. Castro, D. L. John and D. L. Pulfrey, "Towards a compact model for schottky-barrier nanotube FETs," *COMMAD2002*, pp. 303-306.
- [15] D. Basu, M. J. Gilbert, L. F. Register, S. K. Banerjee, A. H. MacDonald, "Effect of edge roughness on electronic transport in graphene nanoribbon channel metal-oxide-semiconductor field-effect transistors," *Appl. Phys. Lett.*, vol. 92, no. 4, p. 042114, 2008.
- [16] S. O. Koswatta, M. S. Lundstrom, and D. E. Nikonov, "Influence of phonon scattering on the performance of p-i-n band-to-band tunneling transistors," *Appl. Phys. Lett.*, vol. 92, p. 043125, 2008.

---

## FIGURE CAPTIONS

- Fig. 1: (a) Schematic cross section of a double-gate (DG) ATB transistor. The channel material is buried between the top and the back oxides with zero thickness. (b) Eigenvalues  $\lambda_n$  and coefficients  $A_n^l$  and  $A_n^r$  in the potential expansion (Eq. (1) and (2)) of a DG GNR SB-FET with  $t_{box} = 50$  nm (SiO<sub>2</sub>),  $t_{tox} = 2.15$  nm (high-k with  $\epsilon_{tox} = 20\epsilon_0$ ), and  $V_{GS} = V_{DS} = 0.3$  V.
- Fig. 2: (a) The extracted effective scaling length  $\lambda_{eff}$ , the lowest order eigenvalue  $\lambda_1$  and the empirical  $\lambda_{emp}$  as a function of  $t_{tox}$  for different  $t_{box}$ . The back oxide is SiO<sub>2</sub> and the top oxide is high-k with  $\epsilon_{tox} = 20\epsilon_0$ . (b)  $\lambda_{eff}$  and  $\lambda_{emp}$  as a function of  $\epsilon_{tox}$  for different  $t_{tox}$ . The back oxide is 50 nm SiO<sub>2</sub>.
- Fig. 3: (a) Calculated transfer characteristics of DG GNR SB-FETs with different gate lengths at  $\lambda_{eff} = 1.45$  nm. Band diagram and current density per energy in the off-state for a DG GNR SB-FET with (b)  $L_g = 10$  nm and (c)  $L_g = 15$  nm, showing that the off-state leakage is dominated by thermionic current at longer channel length (c), and increased dramatically by direct source-to-drain tunneling at short gate length (b) for this geometry ( $\lambda_{eff} = 1.45$  nm).
- Fig. 4: The subthreshold swing ( $SS$ ) vs. (a)  $L_g$ , and (b)  $L_g/\lambda_{eff}$ . For thin  $t_{tox}$  (small  $\lambda_{eff}$ ),  $SS$  significantly increases for  $L_g$  below 15nm due to direct source-to-drain tunneling, while for thick  $t_{tox}$  (large  $\lambda_{eff}$ ),  $SS$  increases to 100mV/dec when  $L_g/(\pi\lambda_{eff}) \approx 1.5$  due to electrostatic short-channel-effects (SCEs), as observed in conventional SOI-MOSFETs [7] [9] [12].

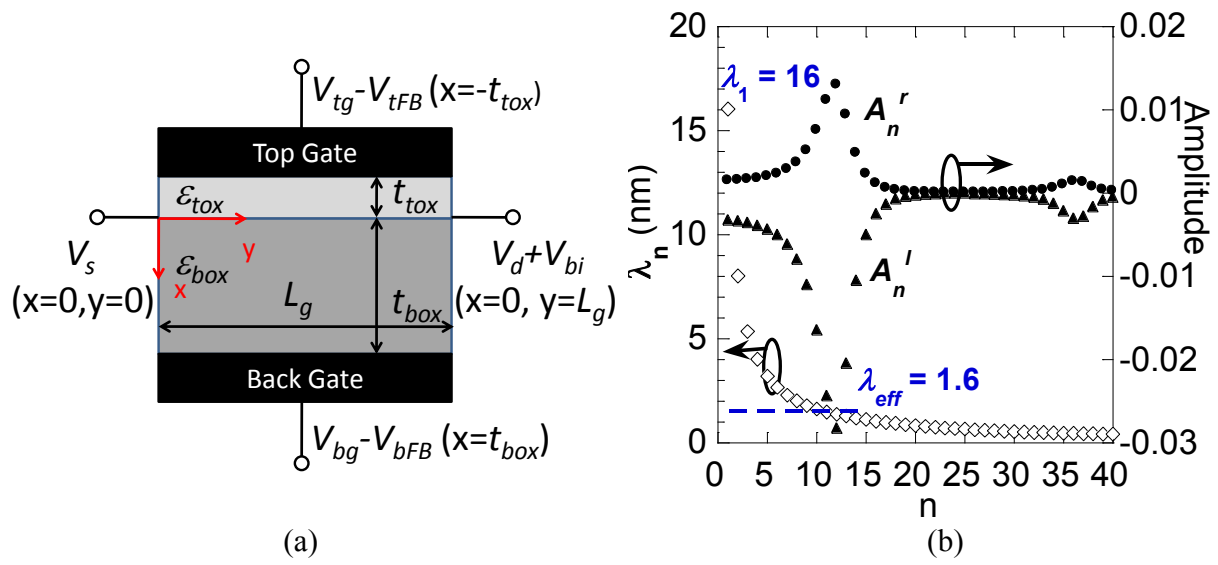


Fig. 1. Q. Zhang, et al., *IEEE Elect. Dev. Lett.*

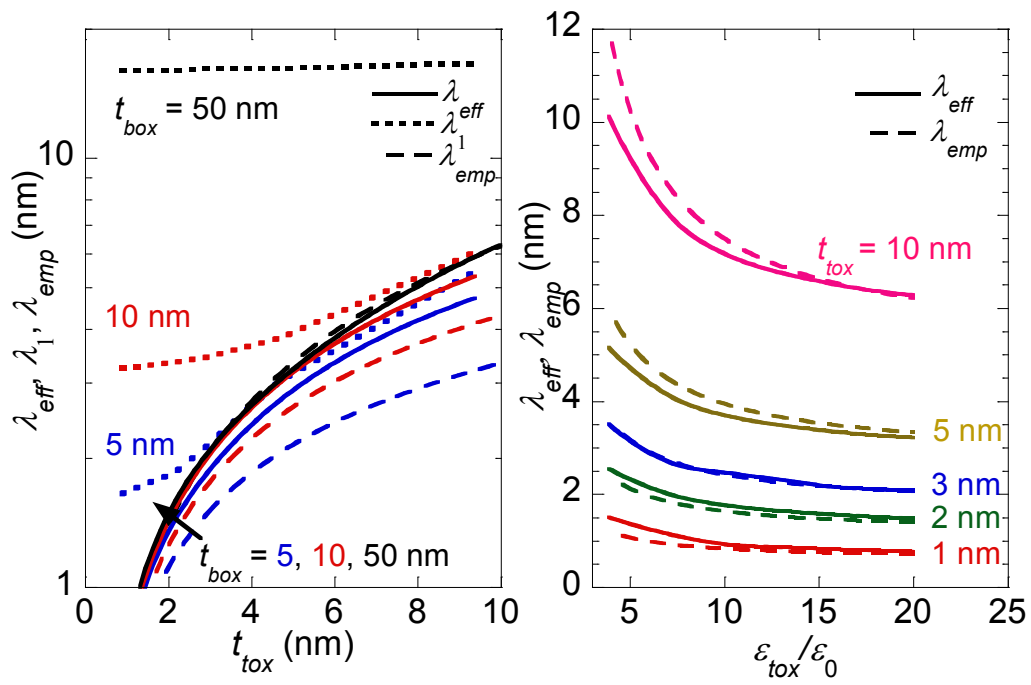


Fig. 2. Q. Zhang, et al., *IEEE Elect. Dev. Lett.*

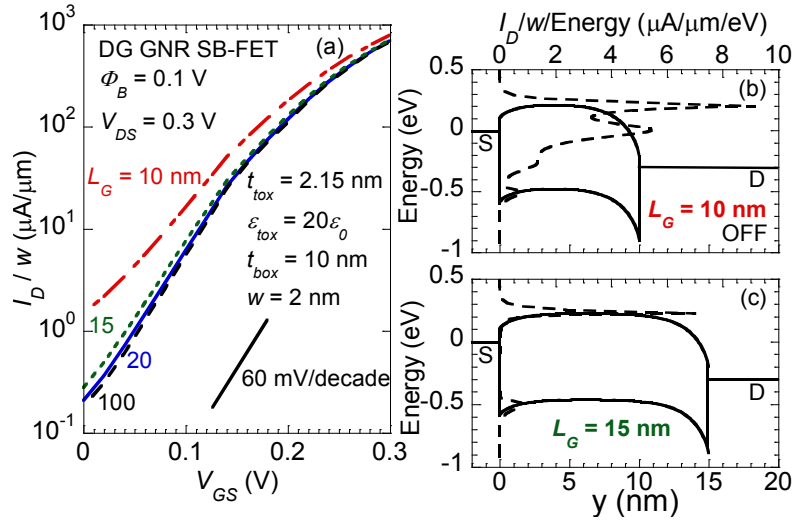


Fig. 3. Q. Zhang, et al., *IEEE Elect. Dev. Lett.*

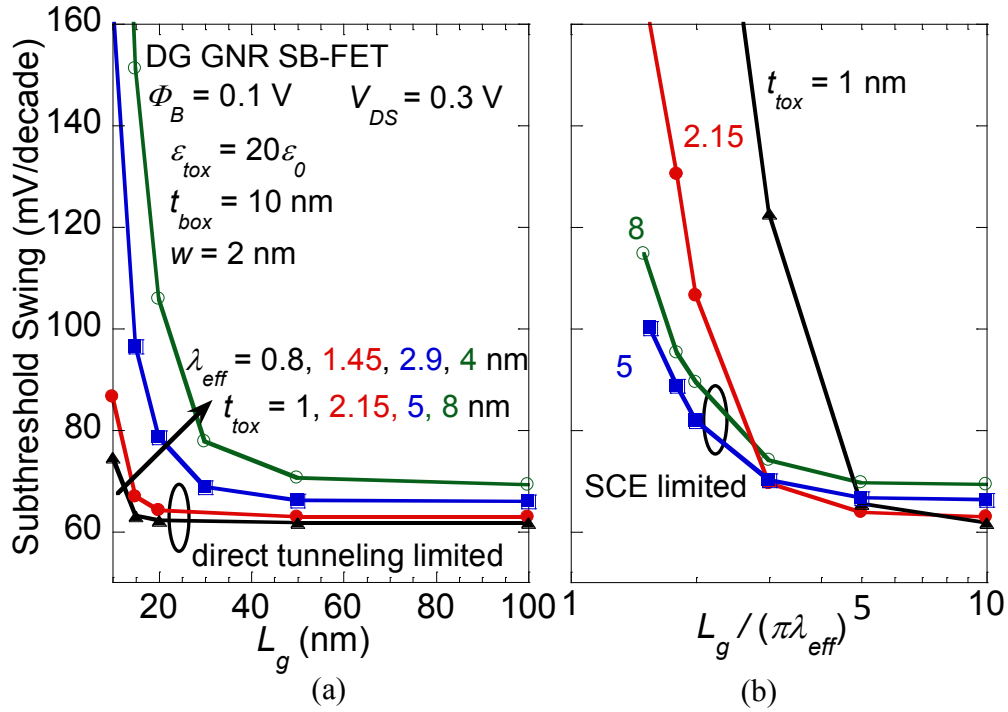


Fig. 4. Q. Zhang, et al., *IEEE Elect. Dev. Lett.*